*Proceedings of the 21st ICSMGE, Vienna, Austria, 14 – 19 June 2026. Pistrol, Adam & Schweiger (eds.)*
*Published by: ÖGG, Austrian Society for Geomechanics, Salzburg, Austria, ISBN 978-3-9503898-4-5*
*https://doi.org/10.53243/ICSMGE2026-1682*

# Constitutive modeling of acid-assisted crack propagation in geomaterials

**Xiaojie Tang**, Jing Chen, Manman Hu*
*Department of Civil Engineering, The University of Hong Kong, Hong Kong, China, mmhu@hku.hk*

ABSTRACT: Controlling environmentally assisted subcritical crack growth plays an essential role in a safe and active geo-energy adaptation to climate change, particularly in the emerging areas of unconventional shale hydrocarbon recovery, Carbon Capture Utilisation and Storage (CCUS), as well as enhanced geothermal systems (EGS). The common feature of these applications is aiming to achieve an enhanced permeability and injectivity in the target formation by the means of hydraulic fracturing. In order to limit the extent of chemical footprint left in the subsurface as well as to ensure the effectiveness of the technique, a sophisticated understanding of the feedback between the mechanics of a geomaterial and the surrounding environment it is subject to is required. We present here constitutive modelling approaches focusing on the effect of an acidic environment on subcritical crack propagation in a stressed geomaterial undergoing mineral dissolution, which depends on the extent of micro-cracking within the process zone. The rate of mineral dissolution is described as a function of acid intensity and a variable specific surface area (SSA) of solid–fluid interface. Our models capture the effect of mineral dissolution on Young's modulus, damage enhancement on chemical softening, as well as a chemically enabled ductilization effect observed in the post-yield behavior of dissolvable rocks. Simulation results also demonstrate that the developed model is capable of reproducing an archetypal three-region behavior of subcritical crack growth in a reactive environment. In parallel, analogue experiments on fluid-driven crack propagation assisted by chemically reactive environment using transparent hydrogels are introduced highlighting an intensified chemical environment acceleration on tensile crack propagation in the subcritical crack growth through chemo-mechanical feedbacks.

KEYWORDS: Chemo-mechanics, mass removal rate, microcracking, ductile behavior, hydrogel.

## 1 INTRODUCTION

To address growing global energy demands, the exploitation of unconventional hydrocarbon reservoirs undergoes rapid development toward commercial viability in recent years. These reservoirs typically comprise tight rock formations with extremely low permeability, where hydrocarbon extraction at economic flow rates proves infeasible without appropriate stimulation techniques (Rahman, 2008). Hydraulic fracturing serves as the predominant stimulation method, involving pressurized water injection to create fracture networks that enhance transport pathways. For carbonate-rich reservoirs, acidizing treatments are frequently integrated to promote subcritical crack propagation at reduced injection pressures (Atkinson, 1984). Despite these advancements, significant challenges persist in optimizing production efficiency while minimizing the environmental impact of these geologically abrupt operations.

Experimental studies on natural calcarenite samples reveal that progressive dissolution under acidic conditions leads to measurable degradation in rock matrix mechanical properties, including strength and deformability characteristics (Ciantia and Hueckel, 2013). Oedometric and triaxial tests have shown that the yield limit of the rock samples is controlled by the variable of reaction progress, through the integrated mass removal. Meanwhile, a chemically induced ductilization effect in the post-yield regime of the rock behaviour is observed in the stress-strain curves (Ciantia et al., 2015a; Ciantia et al., 2015b). A reactive chemo-mechanical model has been recently proposed by the authors (Tang and Hu, 2023) summarizing the observations from the laboratory to describe the response of a geomaterial undergoing chemical softening/weakening in the presence of mineral dissolution. The coupled chemo-mechanical feedback is interpreted as follows. Irreversible damage develops when a geomaterial is severely stressed, which promotes the reaction rate as chemical reaction occurs at available sites on the solid-fluid interface, while micro-cracks contribute to the increase in the specific surface area per unit volume(Tada et al., 1987). Meanwhile, the enhanced dissolution promotes the progressive degradation of the rock skeleton (Hu and Hueckel, 2013). The coupling mechanism of damage-dissolution in the vicinity of crack tip where stress concentrates is supported by an experimental investigation on environmentally assisted cracking using hydrogel as a rock analogue (Chen and Hu, 2024).

In this short paper, we introduce a comprehensive chemo-mechanical modeling framework that incorporates the effect of microcracking-enhanced chemical shrinkage in both elastic and plastic regimes, as well as a chemically induced post-yield ductilization effect. Through analysis of localized mineral dissolution kinetics, we implement a quantity of mass removal rate that captures evolving damage characteristics by employing an adequately scaled REV size. The multi-physics coupling strategy and the governing equations including constitutive considerations in reactive environment, as well as the implementation in an open-source Finite Element simulator are outlined in the paper, followed by numerical investigations on the problem of a single blunt-tip crack propagating into a stressed medium with crack surface subject to fluid pressurization and a long-lasting acid exposure. A short discussion on analogue experiments of fluid-driven crack propagation assisted by chemically reactive environment using transparent hydrogels is followed proving acid-assisted fracturation in a two-way coupling strategy.

## 2 MODEL OUTLINE

### 2.1 *Reactive chemo-visco-plasticity for carbonate rocks in a reactive environment*

The developed reactive elasto-viscoplastic model is outlined below. Laboratory observations suggest that chemically induced alteration on the rock properties occurs in both the elastic and plastic regimes. The rate form of the chemically affected deformation, the total strain rate $\dot{\varepsilon}_{ij}$, is hence decomposed into elastic and plastic components:

$$\dot{\varepsilon}_{ij} = \dot{\varepsilon}_{ij}^{el} + \dot{\varepsilon}_{ij}^{pl} \tag{1}$$

We adopt the chemo-elasticity formulation following (Hu and Hueckel, 2019) and describe the elastic modulus as linearly dependent on the local chemical mass removal:

$$\sigma_{ij} = E_{ijkl}(\xi^{loc}) \cdot \varepsilon_{kl}^{el} \tag{2a}$$

$$\xi^{loc} = \int_0^t \dot{\xi}^{loc} d\tau \tag{2b}$$

where $\sigma_{ij}$ denotes the stress tensor. The elasticity tensor $E_{ijkl}$ is expressed as a function of a scalar variable $\xi^{loc}$ which denotes the time integration of the local mineral mass removal rate $\dot{\xi}^{loc}$.

The irreversible plastic strain rate is assumed to follow an associated flow rule in the following form

$$\dot{\varepsilon}_{ij}^{pl} = \dot{\lambda} \frac{\partial f}{\partial \sigma_{ij}} \tag{3}$$

where $\dot{\lambda}$ denotes a multiplier function representing the rate magnitude, and $\frac{\partial f}{\partial \sigma_{ij}}$ denotes the yield locus gradient which determines the mode of plastic strain rate.

The magnitude of the plastic strain rate is decomposed into deviatoric and volumetric components adopting an extended overstress model, following the strategy proposed in Tang and Hu (2023).

$$\dot{\lambda} = \sqrt{\dot{\varepsilon}_q^{pl\,2} + \dot{\varepsilon}_v^{pl\,2}} \tag{4}$$

where $\dot{\varepsilon}_q^{pl}$ and $\dot{\varepsilon}_v^{pl}$ represent the deviatoric and volumetric components of the plastic strain rate, respectively. In view of the ductile transition in the behavior of rock specimens induced by the chemical process as observed in experiments, an extended overstress model based on the classical model of (Perzyna, 1966) is adopted describing the power-law relationship as

$$\begin{cases} \dot{\varepsilon}_q^{pl} = \dot{\varepsilon}_0 \langle \frac{q - q_Y}{\sigma_{ref}} \rangle^m \\ \dot{\varepsilon}_v^{pl} = \dot{\varepsilon}_0 \langle \frac{p' - p_Y}{\sigma_{ref}} \rangle^m \end{cases} \tag{5}$$

where $\langle \cdot \rangle$ is the Macaulay brackets. $\dot{\varepsilon}_0$ denotes the reference strain rate. $q_Y$ and $p_Y$ are the deviatoric and normal components of the yield stress, respectively. m is the power-law exponent.

Both the deviatoric and normal components of the yield limit are assumed to be dependent on the progress of the damage-enhanced chemical reaction, here represented by the accumulated total mass removal averaged at the REV scale, denoted as $\xi^{REV}$.

$$\begin{cases} q_Y = q_{Y_0}(1 - \beta_q \xi^{REV}) \\ p_Y = p_{Y_0}(1 - \beta_p \xi^{REV}) \end{cases} \tag{6}$$

where $q_{Y_0}$ and $p_{Y_0}$ denote the deviatoric and normal components of the initial yield stress before any chemical weakening, respectively. $\beta_p$ and $\beta_q$ are the corresponding coefficients representing the weakening effect on the deviatoric and normal yield limit components, respectively.

Note that as the process continues with mineral mass gradually removed from the solid matrix considering a reactive environment, the original yield surface (with Drucker-Prager yield criterion for instance) undergoes evolution, corresponding to the alterations of rock cohesion $c$ and friction angle $\varphi$, and a degrading $(p_Y', q_Y)$ as controlled by the chemical weakening law in Eq. (6) with $c = (1 - \beta_q \xi^{REV}) c_0$ and $\mu = \frac{1 - \beta_q \xi^{REV}}{1 - \beta_{p'} \xi^{REV}} \mu_0$. The feedback mechanism featuring the mutually enhancing processes of chemical dissolution and mechanical damage in the crack-tip process zone is expected to accelerate the shrinking of the yield surface as depicted in Fig. 1.

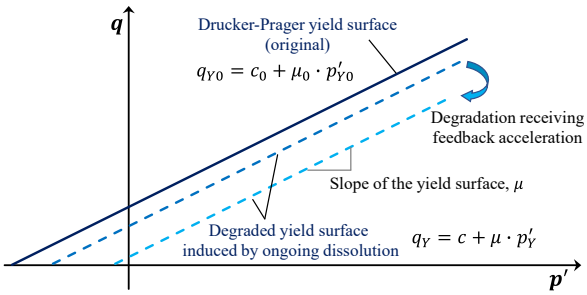


Figure 1. Schematic of Drucker-Prager yield surface in the presence of ongoing chemical mass removal considering a pressure-sensitive rock. Chemically induced shrinking of the yield surface is expected to accelerate due to a two-way feedback mechanism (Tang and Hu, 2025).

We consider that the acidizing is applied to a calcium carbonate rock as a representative for the sake of simplicity for modelling. It is emphasized that the REV-scale variable $\xi^{REV}$ represents the fraction of the dissolved portion over the total soluble mass in the solid matrix, which is thereby bounded by $0 \leq \xi^{REV} \leq 1$. At the upper limit of $\xi^{REV} = 1$, all the dissolvable mass would have been removed from the solid matrix.

The variable $\xi^{REV}$ defines a volume-averaged quantity that encloses the information of the chemical process represented by the local mineral dissolution rate $\dot{\xi}^{loc}$ over time, as well as the damage evolution by taking into account of the additional specific surface area per unit volume generated due to microcracking (Ciantia and Hueckel, 2013; Hueckel and Hu, 2009).

$$\xi^{REV} = \int_0^t (1 + \eta \hat{\varepsilon}) \dot{\xi}^{loc} d\tau \tag{7}$$

where $\eta$ denotes the coefficient of micro-fracturing enhancement on the progress of chemical dissolution and $\hat{\varepsilon}$ denotes a strain invariant acting as a proxy for local mechanical damage.

### 2.2 *Coupled reactive-damage-transport of solute and hydrogen diffusion*

In this study, we consider a typical scenario of calcium carbonate-rich rock subject to a mild acidic environment and assume the dominant chemical reaction is

$$CaCO_3(s) + H^+(aq) \leftrightarrow Ca^{2+}(aq) + HCO_3^-(aq) \tag{8}$$

For a carbonate rock exposed to a chemically reactive aqueous environment with certain acidity, the rate at which calcium carbonate dissolves into the solution depends on the local hydrogen concentration in the fluid phase (Sjöberg and Rickard, 1984). The rate of the calcium mass removed from the rock matrix, as well as the changing rate of $Ca^{2+}$ concentration in the fluid phase is here assumed as a power-law function of local hydrogen concentration. Meanwhile, the mass removal rate has a dependence on the specific surface area per unit volume as described earlier. These two effects are summarized into the reaction term in the reaction-transport equation, which couples the reaction-transport process of $Ca^{2+}$ to the irreversible deformation/damage of the solid matrix and the local acidity. Solute transport of the calcium ion is described by a reactive-diffusive equation with a nonlinear source term from the damage-enhanced dissolution:

$$\partial_t x_{Ca^{2+}} = D_{Ca^{2+}} \nabla^2 x_{Ca^{2+}} + \beta_{H^+}(1 + \eta \hat{\varepsilon})(C_{H^+})^{k'} \tag{9}$$

where $x_{Ca^{2+}}$ denotes the molar fraction of calcium in the fluid phase within the process zone, $D_{Ca^{2+}}$ denoting the diffusivity of

calcium ion, assumed as constant inside the process zone. $\beta_{H^+}$ denotes a lumped constant representing a combined effect of local acidity and damage enhancement on the mass removal rate. The exponent k′ can be assumed as a constant with a value between 0.5~1.0. The evolution of acidity distribution over time is controlled by

$$\partial_t C_{H^+} = D_{H^+}\nabla^2 C_{H^+} - \gamma_{CH}\,\dot{\xi}^{REV} \tag{10}$$

where $C_{H^+}$ indicates the local concentration of hydrogen, $D_{H^+}$ denoting the diffusivity of hydrogen. $\gamma_{CH}$ is a proportionality constant of the mass exchange rate of hydrogen consumption over that of calcium production in the fluid phase.

### 2.3 *Finite element implementation in open-source platform: MOOSE*

Implementation of the reactive-chemo-mechanical model includes a set of inputs and outputs feeding back to the coupled process with key variables. Three physical/chemical processes are explicitly coupled involving enhanced chemical dissolution, solute transport and the evolving mechanical behavior. The final system of Eqs. (1) ~ (10) contains tightly coupled variables, e.g. displacement ($u$), mass removal ($\xi^{\mathrm{loc}}$, $\xi^{\mathrm{REV}}$), hydrogen concentration ($C_{H^+}$) and material properties which can exhibit high nonlinearity in the progressive degradation process.

The proposed reactive-chemo-mechanical model has been implemented in an open-source FEM simulator built on the multiphysics multiscale platform MOOSE (Gaston et al., 2009; Poulet et al., 2017). The final set of governing equations is transformed into a dimensionless group following

$$x^\star = \frac{x}{L_{ref}},\ \sigma^\star{}_{ij} = \frac{\sigma_{ij}}{\sigma_{ref}},\ C^\star = \frac{C}{C_{ref}},\ t^\star = \frac{t}{t_{ref}} \tag{11}$$

where $L_{ref}$, $\sigma_{\mathrm{ref}}$, $C_{ref}$, and $t_{ref}$ represent the reference value of displacement, stress, ion concentration and time, respectively. In this study, the initial radius of the cavity is chosen as the reference length. The reference of concentration is the concentration in a neutral condition where no dissolution occurs. The reference for the stress components is commonly the initial value of rock cohesion. The selection of $t_{ref}$ is made based on $t_{ref} = \frac{L_{ref}^2}{D_{H^+,ref}}$, where $D_{H^+,ref}$ denotes a reference value for the diffusivity of hydrogen. In this study, time reference is defined as 1000 h.

## 3 NUMERICAL SIMULATION: ACID-ASSISTED SUBCRITICAL BLUNT-TIP CRACK PROPAGATION IN CARBONATE ROCKS

### 3.1 *Statement of the problem*

Two-dimensional crack propagation problem as depicted in Fig. 2 is here investigated, where the crack surface is subject to constant hydraulic pressure ($p_{\mathrm{a}}$) and an instantaneously placed long-lasting acid exposure ($C_{\mathrm{H^+|a}}$) simulating the treatment of acidizing, with the exterior boundary under constant overburden pressure ($p_{\mathrm{b}}$). 98876 elements in total were used with mesh size made smaller gradually as is closer to the crack tip surface.

The key parameters are assumed as follows. The ratio of the radius of the exterior boundary over the counterpart of the interior boundary is $\mathrm{b/a} = 15$, the initial Young's modulus $E_0 = 20$ GPa, Poisson ratio $\upsilon = 0.25$, the initial rock cohesion $\mathrm{c_0} = 10$ MPa, $\mathrm{H^+}$ diffusivity $D_{\mathrm{H^+}} = 3.6 \times 10^{-5}$ cm$^2$/s. The von Mises yield criterion is assumed ($\mu = 0$) to simulate pressure insensitive material that the yielding of material occurs when the second invariant of deviatoric stress reaches a critical value. A mild acid condition of pH=5.3 is assumed instantaneously imposed once the mechanical system under the boundary conditions equilibrates itself, which is kept constant on the crack surface afterwards. The hydraulic pressurization acting on the crack surface is assumed to be $p_{\mathrm{a}} = 0.4$ MPa; the exterior is assumed traction-free in the current study, i.e. $p_{\mathrm{b}} = 0$. Reaction-related parameters adopted in this study include $\beta_{p'} = 0$, $\beta_q = 1$, $\eta = 2 \times 10^4$ (Hu and Hueckel, 2013), $k' = 0.9$, $\beta_{\mathrm{H^+}} = 2.5 \times 10^{-3}$ (Ciantia et al., 2015b) unless any of them is a subject of a parametric study. The initial timestep used is 0.01 corresponding to 10 hours in the real. The time step size is reduced by half when the solver fails to obtain a converged solution for a given step. If the solution with the cut-back time step is still unsuccessful, the time step size is repeatedly cut back until a successful solution is obtained. The cut-back step size will be used for the remainder of the computation.

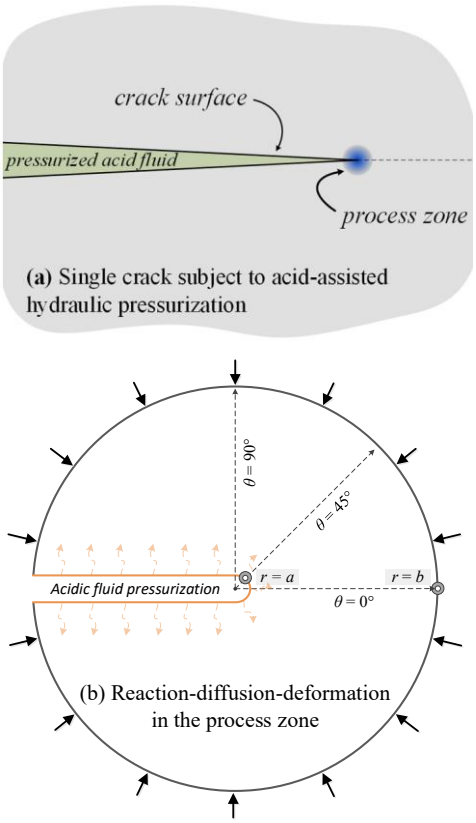


Figure 2. (a) Problem definition of a single crack under coupled hydraulic pressurization and acid diffusion. (b) Model setup of chemically enhanced crack propagation with overburden pressure applied uniformly on the exterior boundary (Tang and Hu, 2025).

### 3.2 *Numerical simulation results*

Figure 3 illustrates the evolution of the radial deviatoric stress distribution along the crack propagation direction during early (several days) and late (more than 1 month) stages. A non-monotonic radial stress profile emerges after 300 h and intensifies in the late stage due to the cumulative effect of chemical degradation accumulating at the crack tip. Quantitatively, the normalized deviatoric stress invariant ($q$/c$_0$) at the tip decreases from 0.936 (t = 300 h) to 0.813 (600 h) and further to 0.544 (900 h), corresponding to progressive mass removal (0.064, 0.187, and 0.456 of the total mass, respectively; see Fig. 4), indicating a chemically driven yielding process.

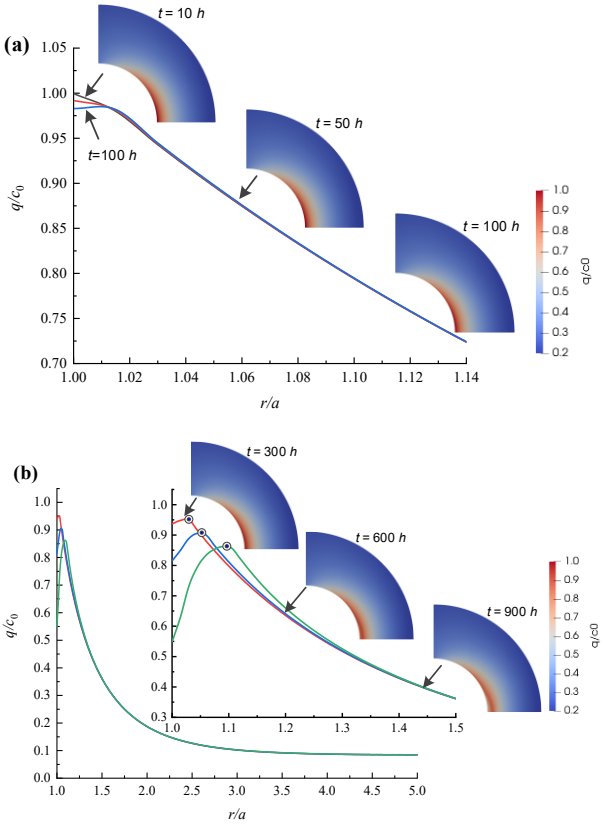


Figure 3. Evolution of the distribution of deviatoric stress normalized by the initial cohesion along the radius at propagation direction (θ=0), upon **(a)** 10, 50, and 100 hours **(b)** 300, 600, and 900 hours of exposure (Tang and Hu, 2024).

At the crack tip, where stress concentrates along the propagation direction, chemical softening is amplified by intensified damage evolution. The progressive increase in specific surface area (SSA) driven by damage generates additional solid-fluid interfaces, creating more sites for mineral dissolution. This leads to an elevated dissolution rate and consequently enhances localized chemical degradation (see Fig. 4). The deviatoric (total) strain contours in Fig. 4 reveal localized damage initiation near the tip under combined acidizing and pressurization, further accelerating mineral dissolution.

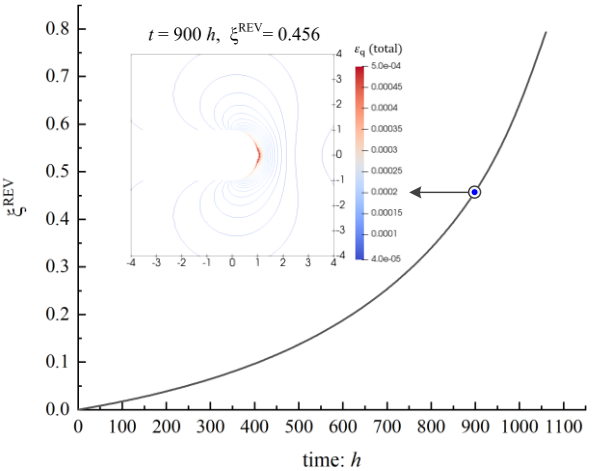


Figure 4. Evolution of the accumulated mass removal at crack tip point during acid pressurization.

Figure 5 demonstrates the influence of acid intensity on crack propagation over time. Lower pH values (indicating higher acidic exposure) accelerate crack growth due to two synergistic mechanisms: 1) damage-enhanced mineral mass removal, 2) intensified chemical degradation in the process zone facilitated by damage evolution. After 1000 hours, cracks propagate more than one order of magnitude further in $pH_a$=5.3 environments compared to $pH_a$=5.6 conditions. This accelerated propagation stems from a mutually enhancement mechanism between chemical mass removal and material degradation, forming a pronounced two-way feedback loop within this dynamically evolving system

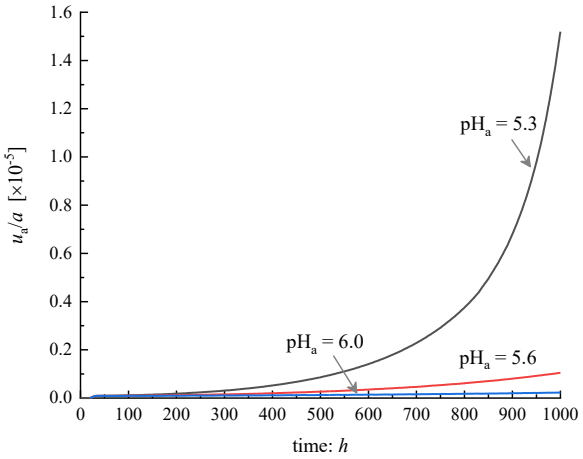


Figure 5. Time evolution of the crack propagation represented by the normalized movement of crack tip point with a variety of acid intensity imposed at cavity wall, for $pH_a = 5.3$, $pH_a = 5.6$, $pH_a = 6.0$, respectively (Tang and Hu, 2024).

Figure 6 presents the logarithmic relationship between crack tip velocity and Mode I (tensile) stress intensity factor ($K_I$) during chemically driven crack propagation ($pH_a$=5.3). Three distinct regimes of crack behavior emerge under chemical loading. For mild acidic conditions ($pH_a$=6.0), the stress intensity factor exhibits insignificant growth with crack extension. Under higher acidity ($pH_a$=5.3), $K_I$ increases more rapidly over time, demonstrating an overall exponential trend, resulting from enhanced degradation of both elastic and plastic mechanical properties near the crack tip, which reduces the strain energy density through combined chemo-mechanical loading.

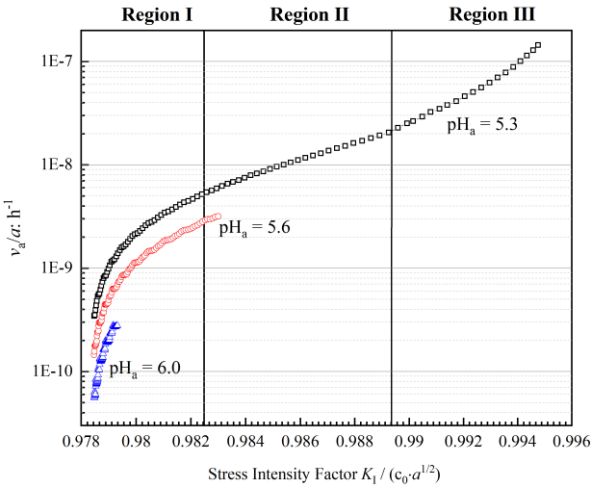


Figure 6. Crack tip velocity (in logarithmic scale) versus Mode I (tensile) stress intensity factor (SIF) $K_I$ at the crack tip with a variety of acid intensity imposed at cavity wall, for $pH_a = 5.3$, $pH_a = 5.6$, $pH_a = 6.0$, respectively.

## 4 DISCUSSION ON ANALOGUE EXPERIMENTS OF FLUID-DRIVEN CRACK PROPAGATION ASSISTED BY CHEMICALLY REACTIVE ENVIRONMENT

An experimental investigation on the effect of a reactive environment on the crack propagation using a Hele-Shaw setup was carried out with alginate hydrogel as an analogue material simulating brittle rocks which is dissoluble upon the exposure to sodium citrate (SC) solutions. More details on the experimental setup and procedures can be accessed in (Chen and Hu, 2024).

Figure 7 exhibits a characteristic three-region development in crack propagation under the three chemical environments, proving our numerical results rational. The imposed chemical environment promotes crack propagation while alleviating the stress concentration at the advancing crack tip, suggesting a more energy-efficient method compared to pure water fracturing. With a higher chemical intensity of the imposed environment, an earlier transition to Region III (the fracturing regime) is expected as the chemical degradation on the toughness of the gel matrix in front of the crack tip meets the threshold value faster in a more reactive environment.

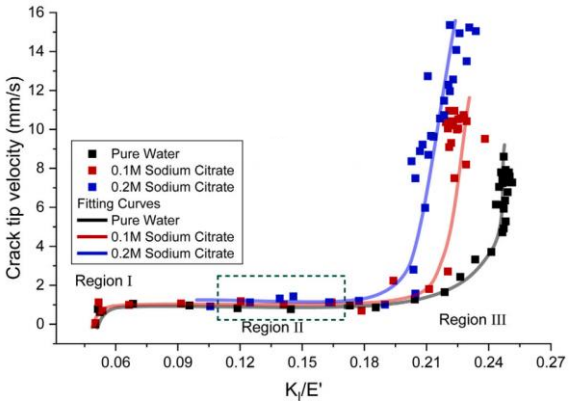


**(a)**

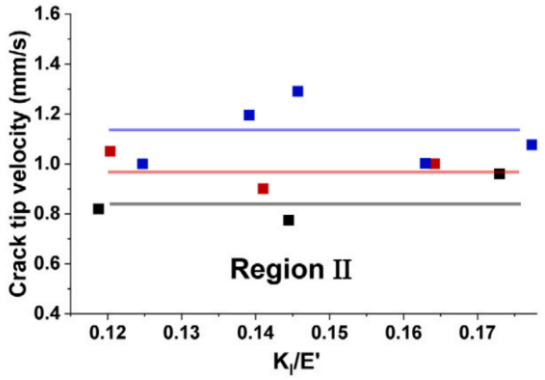


**(b)**

Figure 7. (a) Crack tip velocity versus Mode I (tensile) stress intensity factor (SIF) $K_I$ under different chemical intensities. (b) Magnified view of region II (Chen and Hu, 2024).

## 5 CONCLUSIONS

This paper investigates a fundamental problem of a single crack propagating for pressure-sensitive geomaterial driven by fluid pressurization on the crack surfaces and meanwhile affected by a chemically aggressive environment. A reactive-chemo-mechanical model was formulated which integrates the phenomenological insights on the effect of micro-cracking enhanced chemical degradation in both elastic and plastic domains of rock behavior as well as a chemical ductilization effect in post-yield. Simulation results show that nonlinearity exists in the radial distribution of the deviatoric stress, resulting from the concentrated pressurization in the vicinity of the crack tip, interacting with the damage-influenced mass removal process. Meanwhile, subcritical propagation of a single fracture can be chemically driven and the yielding concentrates at the crack tip forming a localized front penetrating into the exterior area. A typical three-region development of Mode I crack propagation as validated by analogue experiments is revealed by the plotting of crack propagation velocity versus stress intensity factor. The stronger the acid intensity imposed at crack surface, the more accelerated the crack grows.

## 6 ACKNOWLEDGEMENTS

The support by Research Grant Council of Hong Kong (ECS 27203720, GRF 17206521) is acknowledged.

## 7 REFERENCES

Atkinson, B. K. 1984. Subcritical crack growth in geological materials. *Journal of Geophysical Research: Solid Earth*, 89(B6), 4077-4114.

Chen, J., & Hu, M. 2024. Single fluid-driven crack propagation in analogue rock assisted by chemical environment. *Geomechanics for Energy and the Environment*, 37, 100526.

Ciantia, M. O., Castellanza, R., Crosta, G. B., & Hueckel, T. 2015a. Effects of mineral suspension and dissolution on strength and compressibility of soft carbonate rocks. *Engineering Geology*, 184, 1-18.

Ciantia, M. O., Castellanza, R., & di Prisco, C. 2015b. Experimental Study on the Water-Induced Weakening of Calcarenites. *Rock Mechanics and Rock Engineering*, 48(2), 441-461.

Ciantia, M. O., & Hueckel, T. 2013. Weathering of submerged stressed calcarenites: chemo-mechanical coupling mechanisms. *Geotechnique*, 63(9), 768-785.

Gaston, D., Newman, C., Hansen, G., & Lebrun-Grandié, D. 2009. MOOSE: A parallel computational framework for coupled systems of nonlinear equations. *Nuclear Engineering and Design*, 239(10), 1768-1778.

Hu, M., & Hueckel, T. 2013. Environmentally enhanced crack propagation in a chemically degrading isotropic shale. *Geotechnique*, 63(4), 313-321.

Hu, M., & Hueckel, T. 2019. Modeling of subcritical cracking in acidized carbonate rocks via coupled chemo-elasticity. *Geomechanics for Energy and the Environment*, 19, 100114.

Hueckel, T., & Hu, L. B. 2009. Feedback mechanisms in chemo-mechanical multi-scale modeling of soil and sediment compaction. *Computers and Geotechnics*, 36(6), 934-943.

Perzyna, P. 1966. Fundamental Problems in Viscoplasticity. *Advances in Applied Mechanics*, 9, 243-377.

Poulet, T., Paesold, M., & Veveakis, M. 2017. Multi-Physics Modelling of Fault Mechanics Using REDBACK: A Parallel Open-Source Simulator for Tightly Coupled Problems. *Rock Mechanics and Rock Engineering*, 50(3), 733-749.

Rahman, M. 2008. Constrained hydraulic fracture optimization improves recovery from low permeable oil reservoirs. *Energy Sources, Part A*, 30(6), 536-551.

Sjöberg, E. L., & Rickard, D. T. 1984. Temperature dependence of calcite dissolution kinetics between 1 and 62°C at pH 2.7 to 8.4 in aqueous solutions. *Geochimica et Cosmochimica Acta*, 48(3), 485-493.

Tada, R., Maliva, R., & Siever, R. 1987. A new mechanism for pressure solution in porous quartzose sandstone. *Geochimica et Cosmochimica Acta*, 51(9), 2295-2301.

Tang, X., & Hu, M. 2023. A Reactive-Chemo-Mechanical Model for Weak Acid-Assisted Cavity Expansion in Carbonate Rocks. *Rock Mechanics and Rock Engineering*, 56, 515–533.

Tang, X., & Hu, M. 2024. Acid-assisted subcritical blunt-tip crack propagation in carbonate rocks. *Acta Geotechnica*, 19(5), 3095-3113.
Tang, X., & Hu, M. 2025. The Effect of Chemical Environment on Crack Propagation in Pressure-Sensitive Rocks. *Rock Mechanics and Rock Engineering*.